Synthesis of graphene oxide-choline chloride in order to remove phosphate ion from aqueous samples: study of mechanism, isotherm and adsorption kinetics

Thaer Hussein Al-Ameri[1] and Mahnaz Qomi [2],

1-Ministry of Oil / Director of the oil products distribution company/ Najaf Branch (OPDC)

2- Active Pharmaceutical Ingredients Research Center, Pharmaceutical Sciences Branch, Islamic Azad University, Tehran, Iran (APIRC)

Mahnaz.qomi@gmail.com

**Corresponding author : thayralamry536@gmail.com*

Abstract

In this study, a graphene oxide-choline chloride adsorbent was used as a highly efficient and environmentally friendly material for removing phosphate ions from aqueous samples. Graphene oxide was synthesized using the Hummers method and then modified with choline chloride to create the graphene oxide-choline chloride adsorbent. The synthesized adsorbent was characterized using Fourier transform infrared spectrophotometry (FT-IR), Field Effect Scanning Electron Microscopy (FESEM), and Energy-dispersive X-ray spectroscopy (EDX). It was then applied to remove phosphate ions at different pH levels and stirring times. The results of this study showed that the maximum removal efficiency of phosphate ions was achieved at pH 5, with an adsorbent amount of 0.015 g and a stirring time of 30 minutes. Furthermore, it was observed that the adsorption of phosphate ions on the adsorbent surface followed the Langmuir isotherm (monolayer adsorption), with a maximum adsorption capacity of 217.4 mg/g. The examination of absorption kinetics also revealed that the absorption of phosphate ions followed pseudo-second-order kinetics, and an increase in temperature favored the progress of the reaction.

keywords

Graphene oxide-choline chloride, Phosphate removal, Adsorption mechanism, Isotherm , Kinetics

Introduction

Environmental pollution is a result of technological advancements and improper management of resources. Water pollution is caused by various chemicals, including heavy metals, perchlorates, volatile organic compounds, petroleum hydrocarbons, pesticides, pharmaceutical drugs, and waste products from industries and disinfectants (Isiuku and Enyoh, 2020). Nitrates and phosphates, originating from fertilizers, organic manures, and human and animal waste, are major contaminants in water bodies. Chlorides, nitrates, and phosphates are essential anions required for plant growth and are obtained from soil by plants and consumed by humans through diets (Isiuku and Enyoh, 2020). Phosphorus (P) is crucial for the growth and development of organisms and can enter wastewater through sources such as agriculture, pharmaceuticals, paints, and detergents. Phosphate exists in aqueous solutions as orthophosphate and polyphosphate forms (John et al., 2018).

Conventional phosphorus removal technologies, like chemical precipitation and enhanced biological phosphorus removal (EBPR), face challenges in meeting increasingly strict phosphorus regulations, particularly for very low phosphorus concentrations below 0.1 mg P/L (Oehmen et al., 2007). Sorption has emerged as a feasible solution for meeting these stringent standards, and several sorbents have been used for phosphate removal (John et al., 2018). Although progress has been made, further efforts are still required.

In this context, the efficacy of red soil (RS) as an adsorbent for phosphate removal from synthetic and real domestic wastewater was examined. The adsorption of phosphate by RS was found to follow both the Langmuir and Freundlich isotherms. The pseudo-second-order reaction kinetics indicated that both the concentration of the adsorbate and the adsorbent influenced the rate of phosphate adsorption by RS. The intra-particle diffusion model suggested a diffusional nature of the adsorption process, governed by film diffusion and pore diffusion. The results suggest that RS can be a highly favorable and spontaneous low-cost natural adsorbent for phosphate removal from wastewater (Zheng et al., 2020)(Rout et al., 2015).

Graphene oxide has a distinct history that can be understood independently of graphene. Various strong chemical oxidants have been used to synthesize graphene oxide from flake graphite, but its amorphous and complex composition has made understanding its chemical structure an ongoing challenge (Hou et al., 2020). Reduction of graphene oxide to graphene-like materials is a significant chemical transformation that can be achieved chemically, thermally, or electrochemically. The resulting product closely resembles pristine graphene and has shown potential in various physical and engineering applications. Additionally, graphene oxide serves as a useful platform for the fabrication of functionalized graphene platelets, which can enhance mechanical, thermal, and electronic properties. Small molecules and polymers have been covalently or non-covalently attached to graphene oxide for applications such as polymer composites, paper-like materials, sensors, photovoltaics, drug delivery systems, and adsorption (Asgharzadeh and Eslami, 2019, Verma and Nadagouda, 2021).

In this study, graphene oxide-choline chloride was used for the removal of phosphate ions from deionized water and wastewater, with a focus on optimizing the adsorption parameters.

Materials and methods

Sodium hypophosphite (Na_2HPO_3), choline chloride, graphite, hydrogen peroxide (H_2O_2), sodium nitrate ($NaNO_3$), potassium permanganate ($KMnO_4$), nitric acid (HNO_3), and sulfuric acid (H_2SO4) were purchased from Merck and used for subsequent synthesis and processes.

Graphene oxide synthesis

One gram of graphite powder was mixed with 23 milliliters of H_2SO_4 at 5°C for 30 minutes. Then, 0.5 grams of $NaNO_3$ were added to the aforementioned mixture and mixed for 30 minutes at a temperature of 15-20°C while stirring. Next, 3 grams of $KMnO_4$ were added to the mixture and stirred for 90 minutes. The temperature was then raised to 35°C, and the mixture was further mixed for 120 minutes. Afterward, 100 milliliters of deionized water were added, followed by the sudden addition of 5 milliliters of H_2O_2. The final product was washed with deionized water multiple times until the pH of the solution reached approximately 3-4. Finally, it was dried at 60°C for 10 hours (Zhu et al., 2010, Brisebois and Siaj, 2020, Sun, 2019).

Graphene oxide-choline chloride synthesis

First, 0.5 grams of graphene oxide were sonicated with 100 milliliters of deionized water for 1 hour. Then, 0.2 grams of choline chloride were added to the mixture while sonication continued for 20 minutes, followed by additional mixing for 5 hours. Finally, the Graphene oxide-choline chloride adsorbent was washed with deionized water three times and dried at 60°C for 10 minutes (Huang et al., 2015, Lim et al., 2020, Marcano et al., 2010).

A Nicolet 100 Fourier transform infrared (FTIR) spectrometer was used to collect the FT-IR spectroscopic data, which covered the wavelength range of 400–4000 cm^{-1}. To evaluate the morphology of the materials was the scanning electron microscope (SEM) TESCAN VEGAII (Czech Republic). UV-visible spectroscopy was also carried out by UNICO instrument.

Results and discussion

The IR spectra of graphene oxide and Graphene oxide-choline chloride were collected (Figure 1). Accordingly, the peaks at 1050 cm^{-1}, 1220 cm^{-1}, 1650 cm^{-1}, 1730 cm^{-1} and 3500 cm^{-1} correspond to vibrational stretching of C-O, epoxy group, C=C. C=O and O-H, respectively, proving the accuracy of synthesis of graphene oxide (Emily, 2016). On the other hand, compositing of graphene oxide with choline chloride led to declining the intensity of graphene oxide functional groups, illustrating the formation of Graphene oxide-choline chloride.

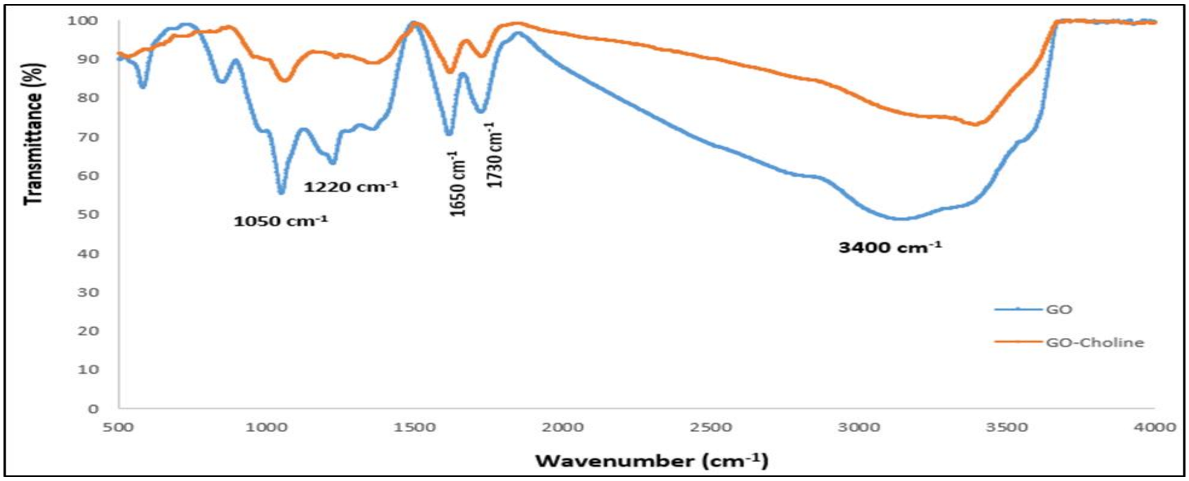

Figure 1 IR spectra of graphene oxide and Graphene oxide-choline chloride

The SEM images of graphene oxide and graphene oxide-choline chloride are shown in (Figure 2). As can be observed, compositing of graphene oxide with choline chloride resulted in wrinkling in graphene oxide sheets which may indicate further interaction of graphene oxide sheets.

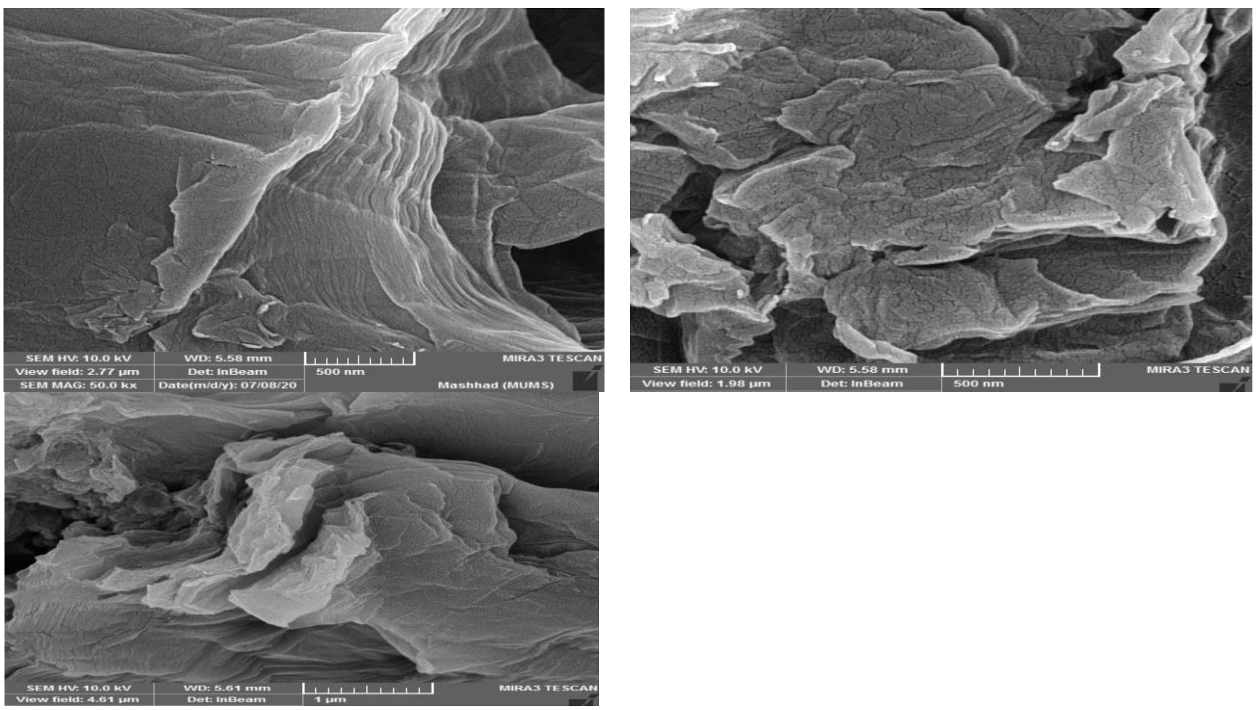

Figure 2 SEM images of graphene oxide and graphene oxide-choline chloride

Moreover, EDAX elemental analysis was also carried out to assess the main elements of graphene oxide-choline chloride, exhibiting peaks related to phosphorus and nitrogen (located at 2.03 and 0.39 eV, respectively). Furthermore, peaks of carbon and oxygen were also observed (i.e., peaks of C and O at 0.28 and 0.52 keV, respectively), indicating the accurate synthesis of the final composite. Please refer to Figure 3 for more details.

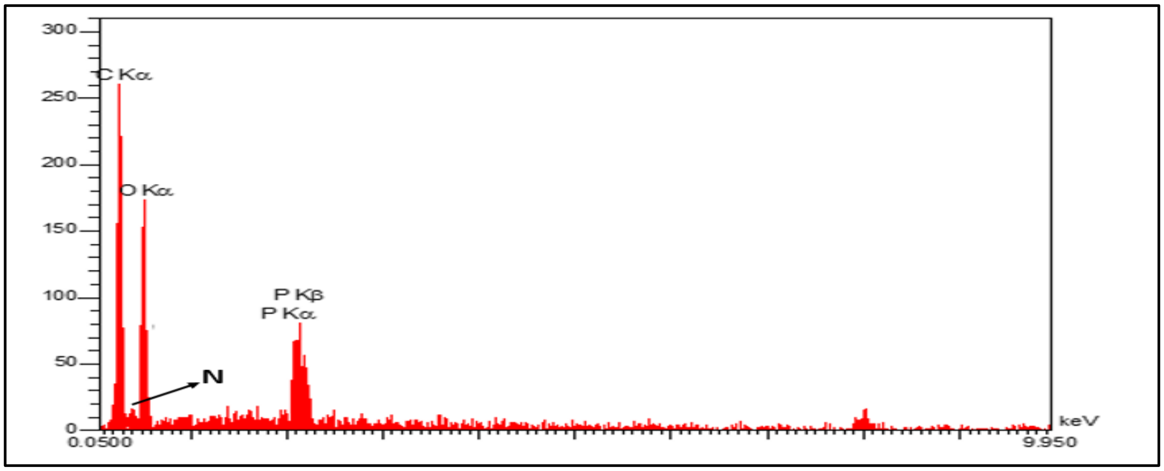

Figure 3 EDAX of graphene oxide-choline chloride

Optimization of parameters

Effect of pH

The pH of solution is a significant factor that affects performance of adsorption. The surface charge of the adsorbent and adsorbate is highly dependent on the pH of the solution. This implies that the deprotonation (or protonation) of an analyte must be considered. The pH can change the ionization degree, the adsorbent surface charge, and the molecular structures of the adsorbate. Therefore, the solution pH determines the type of interaction between the adsorbent and adsorbate through the ionization of species in the solution. Phosphate anion exists in various forms under different pH conditions. In this study, pH of solution was assessed in the range of 2-10, and the highest efficiency was observed at pH 5. The adsorption vs. pH curve was plotted, as shown in Figure 4. In acidic pH, $H_2PO_4^-$ is the dominant group that can interact with the positively charged adsorbent. In basic pH, OH^- anions are competed with the HPO_4^{2-}, leading to a decrease in phosphate ion removal. Therefore, pH of 5 was selected as the optimum pH with the electrostatic attraction during adsorption process.

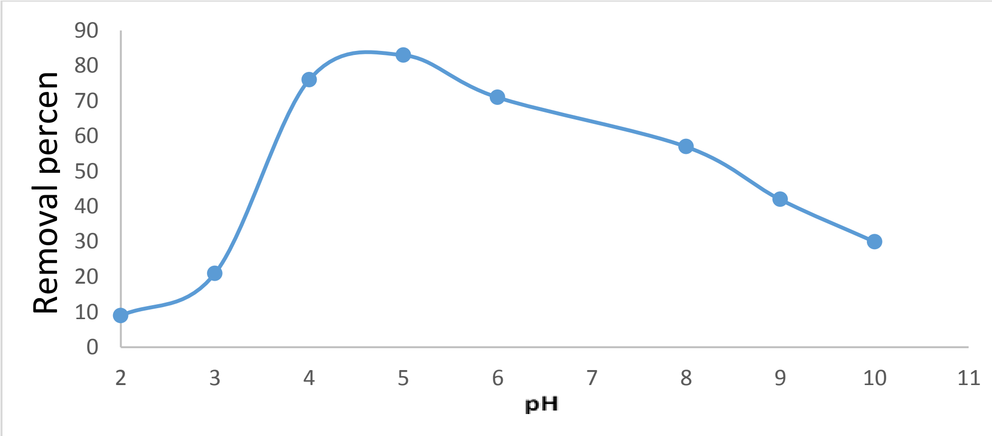

Figure 4 Effect of pH on adsorption efficiency

Adsorption dosage

The adsorbent dosage also affects the adsorption behavior. Generally, increasing the adsorbent dosage leads to an increase the adsorption because more active sites will be accessible for the adsorbate. However, higher dosages may cause adsorbent agglomeration and result in the lose of active sorption sites. As shown in **Figure 5**, increasing adsorption dosage up to 0.015 g results in an increase of adsorption efficiency up to 80% (i.e.50 mg/L). However, further increasing the dosage of adsorption has no significant effect on adsorption efficiency. Therefore, 0.015 g was selected as the optimal amount.

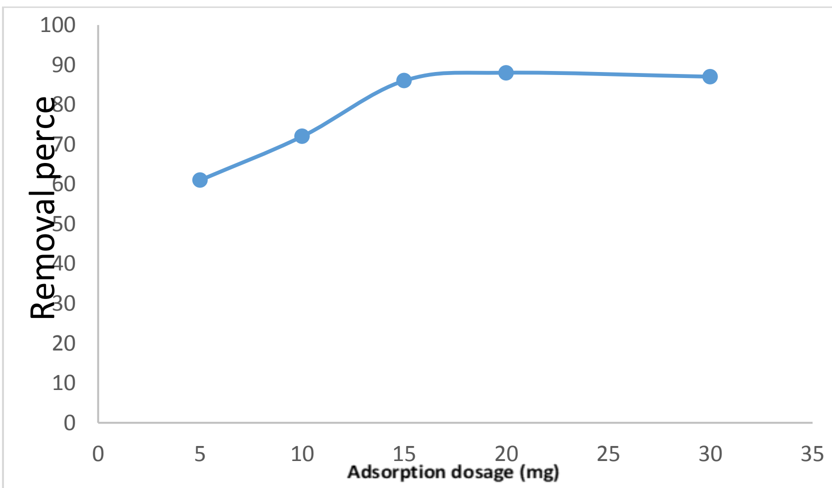

Figure 5 Effect of adsorbent dosage on adsorption efficiency

Contact time

Increasing the contact time can have both negative and positive effects on the adsorptive removal of the adsorbate. The contact between adsorbate and adsorbent is crucial for effective adsorption, as it allows the active sites to interact with the adsorbate. However, when the equilibrium between the sorption sites and anions is established, additional reaction time does not significantly affect adsorption. This is because the sorption sites become saturated during contact time, and no more unoccupied space is available for additional adsorbate. The optimum contact time for phosphate removal is shown in **Figure 6**. In this case, graphene oxide-choline chloride was able to remove the maximum amount of phosphate anion within just 30 minutes.

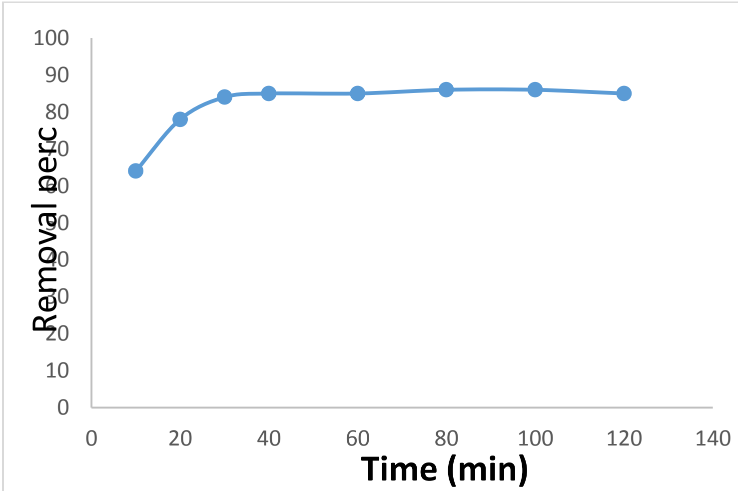

Figure 6 Effect of contact time (min) on adsorption efficiency

Adsorption isotherms

To analyze experimental data from the adsorption process, the distribution of the anions between the aqueous solution and adsorbent at the adjusted temperature is examined to discuss the equilibrium of adsorption. In this regards, some well-known adsorption isotherm equations, including Freundlich, Langmuir, and Temkin will be introduced. Firstly, we present the non-linear form of the Langmuir isotherm as eq. (1):

$$c_e/q_e = c_e/q_{max} + k_L/q_{max} \qquad \text{eq. (1)}$$

where qe (mg/g) represents the equilibrium adsorption capacity and qm (mg/g) is the maximum adsorption capacity. KL (L/mg) denotes the model's constant (Sparks, 2017).

An empirical model for surface heterogeneity and an exponential distribution of energy and sorption sites of the adsorbent is represented by the Freundlich isotherm (Arab et al., 2021). The Freundlich isotherm as a reversible adsorption model is not limited to monolayer formation, It can be described by Eq. (2):

$$\log q_e = \log K_F + \frac{1}{n} \log C_e \qquad \text{Eq. (2)}$$

where K_F (mg/g) and n are described Freundlich constant. The value of n illustrated that the adsorption is favorable and placed in the range of 1 to 10.

The adsorption heat between anions and adsorbent is determined by the Temkin isotherm (Yildirim, 2006). Temkin isotherm assumes an interaction between anions and adsorbent, and it can be presented as Eq (3).

$q_e = {}^{RT}/_{b} \ln(k_T c_e)$ Eq (3)

${}^{RT}/_{b} = B$

Where R is the gas's universal constant (i.e., 8.314 J/mol. K), T (K) is the temperature, bT (J/mol) points to the adsorption heat constant of Temkin and K_T is the Temkin isotherm equilibrium binding constant (L/g).

According to the results, the R^2 value of the Langmuir isotherm for phosphate ions was approximately 0.9906, as shown in Figure 7. This indicates that the Langmuir provided a better fit for the adsorption data, suggesting monolayer uniform adsorption of phosphate onto Graphene oxide-choline chloride without significant interaction between the anions. In comparison, the correlation coefficients of the other two models, namely Freundlich (0.9736) and Temkin (0.9566), were relatively lower than the Langmuir value; as depicted in Figure 8 and Figure 9.

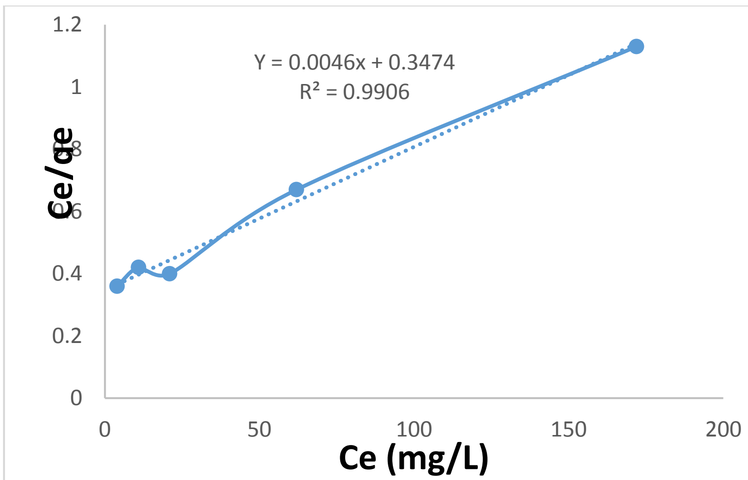

Figure 7 Langmuir isotherm of adsorption

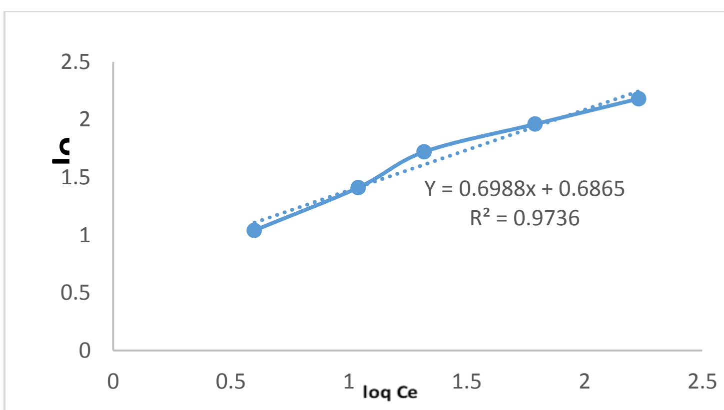

Figure 8 Freundlich isotherm of adsorption

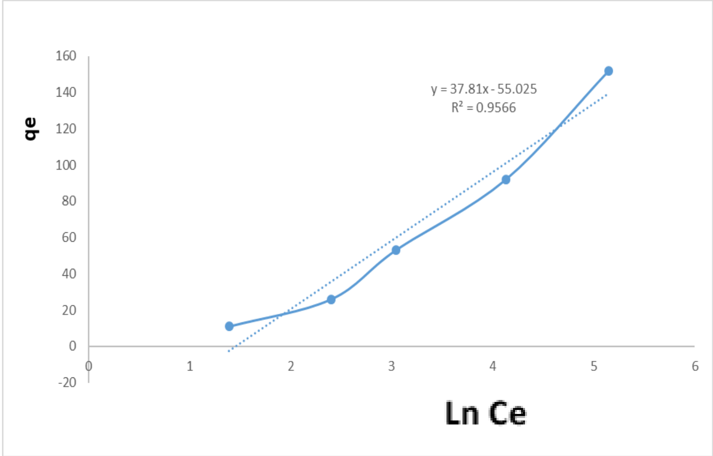

Figure 9 Temkin isotherm of adsorption

Notably, the E value in Temkin isotherm was founded to be lower than 8 (kj.mol^{-1}), indicating that the adsorption of phosphate was of a physical nature on the surface of the adsorbent.

Adsorption kinetics

Kinetic parameters are primarily considered to determine the adsorption efficiency as rapid kinetics is highly significant in aqueous phase adsorption. To assess the kinetic parameters of Graphene oxide-choline chloride, the obtained experimental data were fitted with two commonly used kinetic models: pseudo-first-order and pseudo-second-order kinetic models (Revellame et al., 2020, Christmann, 2013). The pseudo-first-order kinetic model can be represented by Eq. (4):

$$\text{Log}\,(q_e-q_t) = \log q_e - \frac{k_1}{2.303}t \qquad \text{in Eq. (4)}$$

Herein, q_e adsorption capacity in equilibrium, q_t adsorption capacity at time of t in mg/g and k_1 is rate constant of first-order kinetic model (min^{-1}).

The sorption kinetics also was described by the pseudo-second-order model, presented by Eq (5):

$$\frac{t}{qt} = \frac{1}{K_2 qe^2} + \frac{1}{qe}t \qquad \text{in Eq. (5)}$$

Where k_2 is pseudo-second-order model constant (g/mg.min).

Based on results, the R^2 value of pseudo-second-order model for phosphate ions was found to be greater than 0.99 indicating a better fit of the experiments data to this model. The value of R^2 for the pseudo-second-order (R^2> 0.9941) is closer to 1.0 compared to that of the pseudo-first-order model. This demonstrates the suitability of the pseudo-second-order model to describe the rate of adsorption, suggesting that chemisorption may be the rate-limiting step. Consequently, electrostatic attraction interaction plays a significant role in the adsorption process as the subset of the chemisorption category.

Adsorption thermodynamic

Thermodynamic parameters, including Gibbs Free Energy ΔG°, standard entropy ΔS°, and standard enthalpy ΔH°, are calculated using equations 6, 7 and 8, all of which have been described in detail elsewhere (Chen et al., 2015, Sparks, 2003, Christmann, 2013):

$$\text{Ln } K_d = + \frac{\Delta S^{\circ}}{R} - \frac{\Delta H^{\circ}}{RT} \qquad \text{Eq. (6)}$$

$$K_d = \frac{(C_0 - C_e)}{C_0} * \frac{V}{m} \qquad \text{Eq. (7)}$$

$$\Delta G^{\circ} = \Delta H^{\circ} - T\Delta S^{\circ} \qquad \text{Eq. (8)}$$

where K_d points to the distribution coefficient of the adsorption, R and T are the universal gas constant [8.314 J/(mol·K)] and the temperature (K), respectively. Results of tests showed that at 25, 45 and 60 °C, ΔG° values were negative, indicating that the adsorption reaction is thermodynamically spontaneous, see Table 1. Therefore, increasing the temperature can favor of the reaction.

Table 1 Thermodynamic parameters value for the wastewater samples.

Analyte	C_o (mg L^{-1})	ΔH° (kJmol^{-1})	ΔS° (J$mol^{-1}K^{-1}$)	ΔG°, 298.15 K (kJmol^{-1})	ΔG° (318.15) (kJmol^{-1})	ΔG° (333.15) (kJmol^{-1})
	50	-1.781	18.3	-7.23	-7.60	-7.88

Lake water and wastewater were examined to further assess the efficiency of the present method. Since the initial level of phosphate in the lake water in lower that expected, 50 mg/L of phosphate was added to the water to simulate higher levels, and then the adsorption process was carried out. The final efficiency was found to be more than 70%, which is favorable compared with phosphate removal in deionized water.

Conclusions

In conclusion, a composite, consist of graphene oxide and choline chloride was successfully prepared for removal of phosphate ions from deionized water and wastewater. The adsorption behaver of phosphate ions was well described by the Langmuir isotherm, including monolayer adsorption, with a maximum adsorption capacity of 217.4 mg/g. The absorption kinetics followed the pseudo-second-order kinetics model, suggesting that the chemosorption may be the rate-limiting step. Moreover, increasing the temperature was found to be favorable for the progress of the adsorption reaction. The optimum conditions for maximum efficiency were determined as pH 5, an adsorbent dosage of 0.015 g and a stirring time of 30 minutes. These findings demonstrate the potential of the composite material for efficient phosphate removal in water treatment applications.

References

[1] ARAB, K., THOMPSON, D. & OLIVER, I. 2021. Evaluation and characterisation of metal sorption and retention by drinking water treatment residuals (WTRs) for environmental remediation. *International Journal of Environmental Science and Technology*, 1-10.

[2] ASGHARZADEH, H. & ESLAMI, S. 2019. Effect of reduced graphene oxide nanoplatelets content on the mechanical and electrical properties of copper matrix composite. *Journal of Alloys and Compounds,* 806**,** 553-565.

[3] BRISEBOIS, P. & SIAJ, M. 2020. Harvesting graphene oxide–years 1859 to 2019: a review of its structure, synthesis, properties and exfoliation. *Journal of Materials Chemistry C,* 8**,** 1517-1547.

[4] CHEN, H., WANG, X., LI, J. & WANG, X. 2015. Cotton derived carbonaceous aerogels for the efficient removal of organic pollutants and heavy metal ions. *Journal of Materials Chemistry A,* 3**,** 6073-6081.

[5] CHRISTMANN, K. 2013. *Introduction to surface physical chemistry,* Springer Science & Business Media.

[6] EMILY, M. 2016. Fourier Transform Infrared Spectroscopy (FTIR): Methods, Analysis and Research Insights Chemical engineering methods, and technology.

[7] HOU, Y., LV, S., LIU, L. & LIU, X. 2020. High-quality preparation of graphene oxide via the Hummers' method: understanding the roles of the intercalator, oxidant, and graphite particle size. *Ceramics International,* 46**,** 2392-2402.

[8] HUANG, Y., WANG, Y., PAN, Q., WANG, Y., DING, X., XU, K., LI, N. & WEN, Q. 2015. Magnetic graphene oxide modified with choline chloride-based deep eutectic solvent for the solid-phase extraction of protein. *Analytica Chimica Acta,* 877**,** 90-99.

[9] ISIUKU, B. O. & ENYOH, C. E. 2020. Pollution and health risks assessment of nitrate and phosphate concentrations in water bodies in South Eastern, Nigeria. *Environmental Advances,* 2**,** 100018.

[10] JOHN, Y., DAVID, V. E. & MMEREKI, D. 2018. A comparative study on removal of hazardous anions from water by adsorption: a review. *International Journal of Chemical Engineering,* 2018.

[11] LIM, C. Y., MAJID, M. F., RAJASURIYAN, S., MOHD ZAID, H. F., JUMBRI, K. & CHONG, F. K. 2020. Desulfurization performance of choline chloride-based deep eutectic solvents in the presence of graphene oxide. *Environments,* 7**,** 97.

[12] MARCANO, D. C., KOSYNKIN, D. V., BERLIN, J. M., SINITSKII, A., SUN, Z., SLESAREV, A., ALEMANY, L. B., LU, W. & TOUR, J. M. 2010. Improved Synthesis of Graphene Oxide. *ACS Nano,* 4**,** 4806-4814.

[13] OEHMEN, A., LEMOS, P. C., CARVALHO, G., YUAN, Z., KELLER, J., BLACKALL, L. L. & REIS, M. A. M. 2007. Advances in enhanced biological phosphorus removal: From micro to macro scale. *Water Research,* 41**,** 2271-2300.

[14] REVELLAME, E. D., FORTELA, D. L., SHARP, W., HERNANDEZ, R. & ZAPPI, M. E. 2020. Adsorption kinetic modeling using pseudo-first order and pseudo-second order rate laws: A review. *Cleaner Engineering and Technology,* 1**,** 100032.

[15] ROUT, P. R., BHUNIA, P. & DASH, R. R. 2015. A mechanistic approach to evaluate the effectiveness of red soil as a natural adsorbent for phosphate removal from wastewater. *Desalination and Water Treatment,* 54**,** 358-373.

[16] SPARKS, D. L. 2003. *Environmental soil chemistry*, Elsevier.

[17] SPARKS, D. L. 2017. *Environmental soil chemistry*, Academic press.

[18] SUN, L. 2019. Structure and synthesis of graphene oxide. *Chinese Journal of Chemical Engineering,* 27**,** 2251-2260.

[19] VERMA, S. & NADAGOUDA, M. N. 2021. Graphene-Based Composites for Phosphate Removal. *ACS Omega,* 6**,** 4119-4125.

[20] YILDIRIM, E. H. 2006. Surface chemistry of solid and liquid interfaces. *The Journal of Adhesion,* 83**,** 507-508.

[21] ZHENG, Q., YANG, L., SONG, D., ZHANG, S., WU, H., LI, S. & WANG, X. 2020. High adsorption capacity of Mg–Al-modified biochar for phosphate and its potential for phosphate interception in soil. *Chemosphere,* 259**,** 127469.

[22] ZHU, Y., MURALI, S., CAI, W., LI, X., SUK, J. W., POTTS, J. R. & RUOFF, R. S. 2010. Graphene and graphene oxide: synthesis, properties, and applications. *Advanced materials,* 22**,** 3906-3924.

خلاصة

في هذه الدراسة ، تم استخدام مادة أكسيد الجرافين - كلوريد الكولين كمادة ممتزة عالية الكفاءة وصديقة للبيئة لإزالة أيونات الفوسفات من العينات المائية. تم تصنيع أكسيد الجرافين باستخدام طريقة Hummers ثم تم تعديله باستخدام كلوريد الكولين لإنشاء مادة ممتزة من أكسيد الجرافين - كلوريد الكولين. تم تمييز المركبة الممتزة باستخدام مقياس الطيف الضوئي فورييه لتحويل الأشعة تحت الحمراء FT-IR، ومجهر انبعاث المجال الإلكتروني FESEM، و مطيافية تشتت الطاقة بالأشعة السينية . EDX . ثم تم تطبيقه لإزالة أيونات الفوسفات عند مستويات مختلفة من الأس الهيدروجيني وأوقات الرج. أوضحت نتائج هذه الدراسة تحقيق أقصى كفاءة في إزالة أيونات الفوسفات عند درجة حموضة 5 ، بكمية 0.015 جم ووقت الرج 30 دقيقة. علاوة على ذلك ، لوحظ أن امتزاز أيونات الفوسفات على سطح الممتزات يتبع نموذج Langmuir (امتزاز أحادي الطبقة) ، مع قدرة امتزاز قصوى تبلغ 217.4 مجم / جم. كما أظهر فحص حركية الامتزاز أن امتزاز أيونات الفوسفات يتبع الحركية من الدرجة الثانية الزائفة ، وأن الزيادة في درجة الحرارة ساعدت على تقدم التفاعل.